Electrochimica Acta 75 (2012) 332–338

Contents lists available at SciVerse ScienceDirect

Electrochimica Acta

journal homepage: www.elsevier.com/locate/electacta

Synthesis, structure and electrical conductivity of $BaZr_{1-x}Dy_xO_{3-\delta}$ ceramics

Yi-Jing Gu, Zhan-Guo Liu, Jia-Hu Ouyang*, Yu Zhou, Fu-Yao Yan

Institute for Advanced Ceramics, School of Materials Science and Engineering, Harbin Institute of Technology, 92 West Da-Zhi Street, Harbin 150001, China

ARTICLE INFO

Article history:
Received 24 February 2012
Received in revised form 1 May 2012
Accepted 2 May 2012
Available online 8 May 2012

Keywords:
Barium zirconate
Dysprosium oxide
Impedance spectroscopy
Proton conduction
Electrical conductivity

ABSTRACT

Dy^{3+}-doped barium zirconate ceramics, $BaZr_{1-x}Dy_xO_{3-\delta}$ ($x = 0$, 0.05, 0.10, 0.15, 0.20), have been synthesized by pressureless-sintering method at 1973 K for 10 h in air. The structure and electrical conductivity of $BaZr_{1-x}Dy_xO_{3-\delta}$ ceramics were investigated by means of X-ray diffraction, scanning electron microscopy and complex impedance spectroscopy. $BaZr_{1-x}Dy_xO_{3-\delta}$ ceramics exhibit a cubic perovskite structure. The total conductivity of $BaZr_{1-x}Dy_xO_{3-\delta}$ ceramics obeys the Arrhenius relation, and gradually increases with increasing temperature from 723 to 1073 K. The $BaZr_{0.90}Dy_{0.10}O_{3-\delta}$ ceramic exhibits the highest total conductivity at 1073 K. The measured total conductivities of the $BaZr_{0.90}Dy_{0.10}O_{3-\delta}$ ceramic in wet hydrogen (4% H_2O/H_2) and in air are 7.90×10^{-3} S cm^{-1} and 7.31×10^{-3} S cm^{-1} at 1073 K, respectively. The activation energy of $BaZr_{1-x}Dy_xO_{3-\delta}$ ($x = 0.10$, 0.15, 0.20) ceramics is clearly lower than that of undoped $BaZrO_3$ ceramic in both wet hydrogen and air atmospheres, and it can be concluded that the Dy^{3+}-doped $BaZr_{1-x}Dy_xO_{3-\delta}$ ($x = 0.10$, 0.15, 0.20) ceramics are potential proton conductors.

1. Introduction

Solid oxide fuel cells (SOFCs) are considered as the fourth power generation technology, which have the high energy conversion efficiency and a low impact on the environment [1–4]. They are composed of cathodes, electrolytes and anodes [5–8]. Generally, the electrolyte is the key to determine the operating temperature, which includes oxide-ion electrolytes [9] and proton conducting electrolytes [10]. The SOFCs with proton conducting electrolytes can operate at lower temperatures than those conventional SOFCs with oxide-ion electrolytes [10]. Perovskite-type proton conductor is considered to be a potential candidate for applications in hydrogen sensors [11] and hydrogen pumps [12].

$BaZrO_3$ doped with trivalent rare earth or bivalent alkaline earth metallic oxides has the ability of high proton conductivity with excellent chemical stability [10,13]. If the tetravalent cation Zr^{4+} at the B-site is partially substituted by the trivalent rare-earth metallic cation, oxygen vacancies may be formed as the following Eq. (1) [14].

$$2Zr_{Zr}^{X} + Y_2O_3 + O_O^{X} \rightarrow 2Y'_{Zr} + V_O^{\bullet\bullet} + 2ZrO_2 \qquad (1)$$

Proton defects occur under the condition of gas phase water existing. The hydroxide anion from gas water fills into oxygen vacancies, and the proton forms a covalent bond with lattice oxygen [10]. Thus, two proton defects are formed. As the proton is the smallest carrier, the activation energy of proton conductor is about 0.4–0.6 eV [15], which is much lower than that of oxide-ion conductor, such as YSZ and the doped ceria [16]. Among proton conductors, the trivalent rare-earth metallic cation is generally used to dope at the B-site [17–19], while the divalent alkaline-earth metallic cation is at the A-site [20]. It is the common opinion that yttrium oxide is the best doping oxide for $BaZrO_3$-based electrolytes [21–24]. Normally, the doping content of yttrium oxide into barium zirconate is less than 0.2 [23,25–27]. Fabbri et al. also investigated the influence of Y^{3+}-dopant content on the proton conductivity of $BaZr_{1-x}Y_xO_{3-\delta}$ ($0.2 \le x \le 0.5$) fuel cell electrolytes, however, they found that the highest electrical conductivity is obtained at $x = 0.2$ [28]. The ionic radius of Dy^{3+} at the B-site of the perovskite-type structure is 0.0912 nm, which is quite similar to that of Y^{3+} cation (0.090 nm) [29]. Dy^{3+}-doped $BaZrO_3$-based electrolytes has attracted great attention on the improvement of the electrical conductivity.

In the present work, $BaZr_{1-x}Dy_xO_{3-\delta}$ ($x = 0$, 0.05, 0.10, 0.15, 0.20) ceramics were prepared for the first time via conventional solid state reaction method. The objective of this work is to investigate the influence of the Dy^{3+}-dopant content on the structure and electrical conductivity of $BaZr_{1-x}Dy_xO_{3-\delta}$ ceramics.

2. Experimental procedure

$BaZr_{1-x}Dy_xO_{3-\delta}$ ($x = 0$, 0.05, 0.10, 0.15, 0.20) powders were synthesized by high-temperature solid state reaction method. $BaCO_3$ (Tianjin Kermel Chemical Reagent Co., Ltd., China; purity ≥ 99%), ZrO_2 (Dongguan SG Ceramics Technology Co., Ltd., China; purity ≥ 99.9%), Dy_2O_3 (Rare-Chem Hi-Tech Co., Ltd., China; purity ≥ 99.99%) powders were used as raw materials, and were weighed in stoichiometric proportions according to the molecular

---

* Corresponding author. Tel.: +86 451 86414291; fax: +86 451 86414291.
E-mail address: ouyangjh@hit.edu.cn (J.-H. Ouyang).

0013-4686/$ – see front matter © 2012 Elsevier Ltd. All rights reserved.
http://dx.doi.org/10.1016/j.electacta.2012.05.002

formula after being calcined at 1173 K for 2 h in air in order to make sure the exact weighing. The starting powders were milled for 24 h in pure ethanol with zirconia balls and the weight ratio of powders and zirconia balls was 1:2.5. Then the mixed powders were dried in an oven and calcined at 1523 K for 10 h. The obtained powders were uniaxially pressed into pellets at 20 MPa after grinding in an agate mortar, and were subsequently cold isostatically pressed at 400 MPa for 5 min. The pellets were pressureless-sintered at 1973 K for 10 h in air at the heating rate of 4 K min^{-1}.

The phase identification of $BaZr_{1-x}Dy_xO_{3-\delta}$ ($x = 0, 0.05, 0.10, 0.15, 0.20$) ceramics was performed by an X-ray diffractometer (Rigaku D/Max 2200VPC, Japan) with Ni filtered Cu Kα radiation after all the pellets were polished. The XRD patterns were recorded in the 2θ range of 10–70° at a scanning rate of 5° min^{-1} in air at room temperature. The instrument was calibrated using the pure silicon sample provided with the instrument. The density of sintered samples was measured by Archimedes method. The theoretical density of each composition was calculated using lattice parameters acquired from the XRD results and the molecular weight in an elementary cell. The surface morphology of the sintered samples was examined by a field-emission scanning electron microscope (SEM, FEI Quanta 200F, The Netherlands) equipped with an energy dispersive X-ray (EDX) spectroscopy analyzer with an accelerating voltage of 20 kV. For SEM observations, the specimens were polished with 1 μm diamond paste, and then thermally etched at 1873 K for 1 h in air before a thin electricity-conductive coating was evaporated onto the surfaces of specimens.

The electrical conductivity of $BaZr_{1-x}Dy_xO_{3-\delta}$ ceramics was investigated at intermediate temperatures of 723–1073 K in both wet hydrogen (4% H_2O-saturated H_2) and ambient air atmospheres by AC impedance spectroscopy using the four-point probe technique with an impedance/gain-phase analyzer through a dual channel potentiostat instrument (VSP, France) in the frequency range from 0.5 Hz to 1 MHz. The data analysis was carried out by Zview 2 software with appropriate equivalent circuits. All the specimens for electrochemical measurements were polished into the regular discs with the thickness of about 3.0 mm. Both sides of every sample with an area of 0.28 cm^2 were coated with silver paste to form the electrode. In order to investigate the influence of the water vapor on the electrical conductivity, the samples were carefully prepared for evaluation under different measurement conditions of 4% H_2O/H_2, 10% H_2O/H_2 and 20% H_2O/H_2 atmospheres, respectively.

3. Results and discussion

3.1. Structural analysis of $BaZr_{1-x}Dy_xO_{3-\delta}$ ceramics

The X-ray diffraction patterns of $BaZr_{1-x}Dy_xO_{3-\delta}$ ($x = 0, 0.05, 0.10, 0.15, 0.20$) ceramics sintered at 1973 K for 10 h are shown in Fig. 1. All $BaZr_{1-x}Dy_xO_{3-\delta}$ ceramics exhibit a single cubic perovskite-type structure. All the peaks with Miller indices ($h\,k\,l$) are matching well with the standard XRD card of barium zirconate (JCPDS file no. 06-0399) without any impurity phase. With increasing the Dy^{3+}-doped content, all the peaks of $BaZr_{1-x}Dy_xO_{3-\delta}$ ceramics shift to the low angle side as compared with those of undoped $BaZrO_3$ ceramics, implying that Dy^{3+} doping into $BaZrO_3$ leads to a larger lattice parameter. It is due to the larger ionic radius of Dy^{3+} (0.0912 nm) than that (0.072 nm) of Zr^{4+} cation [29]. After the Dy^{3+} cation occupies the Zr^{4+} site of perovskite structure, the lattice parameter becomes larger, as shown in the following Eq. (2)

$$Dy_2O_3 \rightarrow 2Dy'_{Zr} + V_O^{\bullet\bullet} + 3O_O^X \qquad (2)$$

From the measured XRD patterns, the derived lattice parameters are shown in Fig. 2, which obeys Vegard's law. The unit cell volumes and the relative densities are presented in Table 1. Clearly, the unit cell volume increases with increasing the Dy^{3+}-dopant content. The relative density of $BaZr_{1-x}Dy_xO_{3-\delta}$ ceramics is between 91% and 95%, and decreases with increasing the Dy^{3+}-dopant content.

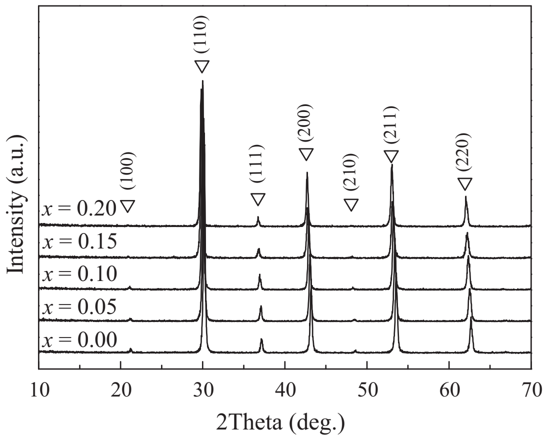

Fig. 1. XRD patterns of $BaZr_{1-x}Dy_xO_{3-\delta}$ ($x = 0, 0.05, 0.10, 0.15, 0.20$) ceramics sintered at 1973 K for 10 h.

The microstructure of $BaZr_{1-x}Dy_xO_{3-\delta}$ ($x = 0, 0.05, 0.10, 0.15, 0.20$) ceramics sintered at 1973 K for 10 h are shown in Fig. 3. Clearly, the morphologies of undoped and Dy^{3+}-doped barium zirconates are quite different, however, the morphologies of $BaZr_{1-x}Dy_xO_{3-\delta}$ ($x = 0.05, 0.10, 0.15, 0.20$) ceramics are very similar as shown in Fig. 3(b)–(e). The grains are closely packed, and the grain boundaries are very clean. All the examined samples are with a single phase, and there exists no second phase. From Fig. 3, there is almost no open porosity in the sintered samples. It is worth mentioning that these micrographs are well accorded with the XRD results. Clearly, all the Dy^{3+}-doped barium zirconates, $BaZr_{1-x}Dy_xO_{3-\delta}$ ($x = 0, 0.05, 0.10, 0.15, 0.20$), form a single cubic phase. The Dy^{3+}-dopant seems to cause a slight growth of grains in sintered ceramics, in comparison with undoped barium zirconate. The grain size is approximately 1–3 μm at $x = 0.05$. However, as the Dy^{3+}-dopant content increases from 0.05 to 0.20, the grain size is clearly larger than that at $x = 0.05$, as shown in Fig. 3(b)–(e).

3.2. Electrical conductivity of $BaZr_{1-x}Dy_xO_{3-\delta}$ ceramics

The complex impedance plots of the $BaZr_{0.90}Dy_{0.10}O_{3-\delta}$ ceramic at temperatures of 723–823 K in the atmosphere of wet hydrogen (4% H_2O-saturated H_2) are shown in Fig. 4. The complex impedance plot consists of three contributions commonly, which are the grain

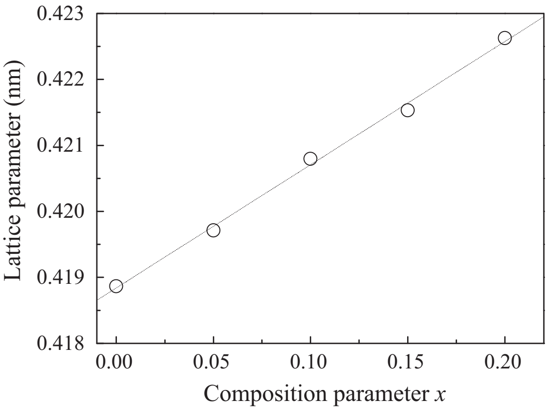

Fig. 2. Derived lattice parameters of $BaZr_{1-x}Dy_xO_{3-\delta}$ ($x = 0, 0.05, 0.10, 0.15, 0.20$) ceramics sintered at 1973 K for 10 h.